

1       **Optimization of a chemical scrubbing process based on a Fe-EDTA-**  
2       **carbonate based solvent for the simultaneous removal of CO<sub>2</sub> and H<sub>2</sub>S**  
3                               **from biogas**

4       David Marín<sup>1, 2, 3</sup>, Marisol Vega<sup>2, 4</sup>, Raquel Lebrero<sup>1, 2</sup>, Raúl Muñoz<sup>\*1, 2</sup>

5       <sup>1</sup>Department of Chemical Engineering and Environmental Technology, School of Industrial Engineering,  
6       Valladolid University, Dr. Mergelina, s/n, 47011, Valladolid, Spain.

7       <sup>2</sup>Institute of Sustainable Processes, Dr. Mergelina, s/n, 47011, Valladolid, Spain.

8       <sup>3</sup>Universidad Pedagógica Nacional Francisco Morazán, Boulevard Centroamérica, Tegucigalpa, Honduras.

9       <sup>4</sup>Department of Analytical Chemistry, University of Valladolid, Campus Miguel Delibes, Paseo Belén 7,  
10      47011 Valladolid, Spain.

11

12      \* Corresponding author: mutora@iq.uva.es

13

14      **ABSTRACT**

15      The potential of a novel Fe/EDTA/carbonate-based scrubbing process for the  
16      simultaneous removal of H<sub>2</sub>S and CO<sub>2</sub> from biogas was studied by evaluating the  
17      influence of Fe/EDTA molarity (M), carbonate concentration (IC), biogas (B), air (A) and  
18      liquid (L) flow rates on biogas upgrading performance using a Taguchi L<sub>16</sub>(4<sup>5</sup>)  
19      experimental design. The ANOVA demonstrated that molarity of the Fe/EDTA solution  
20      was a significant factor influencing H<sub>2</sub>S concentration (0.035% at 0.00M to 0.000% at  
21      0.05M). IC impacted on the concentrations of CO<sub>2</sub> (13.1 and 4.5% at 4000 and 10000mg  
22      IC L<sup>-1</sup>, respectively), N<sub>2</sub> and CH<sub>4</sub> (85.9 and 94.5% at 4000 and 10000mgIC L<sup>-1</sup>,  
23      respectively). The biogas flow rate affected the concentrations of CO<sub>2</sub> (2.5 to 13.8% at  
24      10 and 40mL min<sup>-1</sup>, respectively), O<sub>2</sub>, N<sub>2</sub> and CH<sub>4</sub> (95.9 to 85.4% at 10 and 40mL min<sup>-1</sup>,  
25      respectively). Likewise, the recycling liquid flow rate affected CO<sub>2</sub> (8.3 and 5.9% at 5  
26      and 30mL min<sup>-1</sup>, respectively), O<sub>2</sub>, N<sub>2</sub> and CH<sub>4</sub> (90.5 and 93.3% at 5 and 40mL min<sup>-1</sup>,

27 respectively) concentrations. Finally, the air flow rate impacted on CO<sub>2</sub> (10.8 and 6.7%  
28 at 800 and 1000mL min<sup>-1</sup>, respectively), H<sub>2</sub>S, N<sub>2</sub> and CH<sub>4</sub> (87.9 and 92.2% at 800 and  
29 1000mL min<sup>-1</sup>, respectively) concentrations. Process optimization provided the optimal  
30 conditions for each control factor. Continuous biogas upgrading operation at M<sub>2</sub>-IC<sub>1</sub>-B<sub>2</sub>-  
31 A<sub>4</sub>-L<sub>4</sub> (0.05M, 10000mgIC L<sup>-1</sup>, 10mL min<sup>-1</sup>, 1000mL min<sup>-1</sup> and 30mL min<sup>-1</sup>,  
32 respectively) provided CH<sub>4</sub>, CO<sub>2</sub>, O<sub>2</sub>, N<sub>2</sub> and H<sub>2</sub>S concentration in the upgrading biogas  
33 of 97.4, 1.4, 0.29, 0.97 and 0%, respectively, which complied with biomethane  
34 regulations.

35

36 **Keywords:** Absorption-stripping process; Biogas upgrading; Biomethane; Chemical  
37 scrubbing; Taguchi's design.

38

### 39 **1. Introduction**

40 Biogas from anaerobic waste treatment represents a renewable energy vector that can be  
41 used as a fuel to power vehicles or to generate electricity and heat for domestic and  
42 industrial applications, which can partially mitigate Europe's dependence on imported  
43 fossil fuels [1,2]. In this context, the number of biogas plants in Europe has increased  
44 from 6227 in 2009 to 17783 by the end of 2017, while biomethane production capacity  
45 has also increased from 752 GWh in 2011 to 19352 GWh by the end of 2017 [3]. An  
46 upgrading of biogas into biomethane is required prior use as a vehicle fuel or for the  
47 injection into natural gas grids due to the high concentration of impurities present in raw  
48 biogas: CO<sub>2</sub> (15-60%), CO (<0.6%), H<sub>2</sub>S (0.005-2%), N<sub>2</sub> (0-2%), O<sub>2</sub> (0-1%), NH<sub>3</sub>  
49 (<1%), siloxanes (0-0.2%) and volatile organic compounds (<0.6%) [4]. Hence, most  
50 international biomethane standards require a composition of CH<sub>4</sub> ≥ 90-95%, CO<sub>2</sub> ≤ 2-  
51 4%, O<sub>2</sub> ≤ 1% and negligible amounts of H<sub>2</sub>S [2,5,6].

52

53 Multiple technologies are nowadays commercially available or under validation phase to  
54 remove CO<sub>2</sub> and H<sub>2</sub>S from biogas in order to fullfil with biomethane standards.  
55 Biological technologies are being succesfully scaled-up since the past decade and exhibit  
56 lower environmental impacts and lower operating costs. However, biotechnologies  
57 require either a cost-effective H<sub>2</sub> production from renewable energy surplus (in the case  
58 of hydrogenotrophic upgrading) or large areas and favourable environmental conditions  
59 (in the case of photosynthetic biogas upgrading) [2,7]. On the other hand, membrane  
60 separation, chemical/water/organic scrubbing, cryogenic separation or pressure swing  
61 adsorption can remove CO<sub>2</sub> from biogas, while *in-situ* chemical precipitation or  
62 adsorption onto activated carbon or metal ions provide an effective H<sub>2</sub>S removal [2,7].  
63 These physicochemical methods present high operating costs (2-5 ct€ kWh<sup>-1</sup>) and  
64 environmental impacts as a result of their high energy demand, entail process operation  
65 at high temperatures and pressures, and can not support a simultaneous H<sub>2</sub>S and CO<sub>2</sub>  
66 removal [8]. Therefore, there is an urgent need to develop cost-effective technologies  
67 operating under ambient conditions capable of supporting an integral biogas upgrading  
68 (H<sub>2</sub>S and CO<sub>2</sub> removal in a single step process), which will increase the environmental  
69 and economic sustainability of biogas upgrading and boost biomethane industry.

70

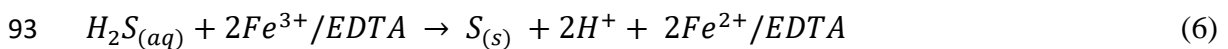
71 In this context, the use of an absorption-stripping process based on an aqueous solution  
72 of Fe-EDTA-carbonate represents an innovative physicochemical technology capable of  
73 simultaneously removing H<sub>2</sub>S and CO<sub>2</sub> from biogas [9]. Highly carbonated aqueous  
74 solutions at high pH mediate a rapid and effective CO<sub>2</sub> capture at ambient pressure and  
75 allow an air-aided CO<sub>2</sub> desorption. The absorption and dissociation of CO<sub>2</sub> is described  
76 by equations (1) to (4):



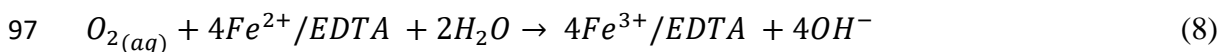
81 The mass transfer of CO<sub>2</sub> from the biogas to the aqueous chemical solution can be  
 82 described as a function of a volumetric mass transfer coefficient (k<sub>LA</sub>), multiplied by the  
 83 concentration gradient in the liquid phase ( $\frac{CO_{2g}}{H} - CO_{2L}$ ), where H is the dimensionless  
 84 Henry's law constant. At this point it should be stressed that the high pH of the scrubbing  
 85 solution maintains the value of CO<sub>2L</sub> very low, and therefore, the gas-liquid concentration  
 86 gradient as a maximum value. In addition, the high ionic strength of the scrubbing  
 87 solution prevents the coalescence of biogas bubbles, which enhances k<sub>LA</sub>.

88

89 On the other hand, Fe<sup>3+</sup>-EDTA solutions support a cost effective H<sub>2</sub>S oxidation to  
 90 elemental sulphur. According with Wubs and Beenackers [10], the absorption and  
 91 oxidation of H<sub>2</sub>S with Fe-EDTA is described by equations (5) and (6):



94 The Fe<sup>2+</sup>/EDTA resulting from H<sub>2</sub>S oxidation to S can be regenerated into its active ferric  
 95 form (Fe<sup>3+</sup>/EDTA) by oxidation with the air used for CO<sub>2</sub> stripping (equations 7 and 8).



98 Several studies have investigated the potential of Fe<sup>3+</sup>/EDTA to remove H<sub>2</sub>S from biogas.

99 In this sense, Horikawa et al., [11] studied the purification of biogas and reported a 90%

100 removal of H<sub>2</sub>S from biogas using a 0.2 M Fe/EDTA aqueous solution in a system

101 composed of an absorption and a regeneration column with a total volume of 0.82 L.  
102 Similarly, Schiavon Maia et al., [12] observed a 91% removal of H<sub>2</sub>S in a similar  
103 absorption-regeneration system using a 0.2 M Fe/EDTA solution, at biogas and liquid  
104 flow rates of 340 mL min<sup>-1</sup>. Finally, Frare et al., [13] investigated the absorption  
105 efficiency of H<sub>2</sub>S in a similar absorption-regeneration system using a 0.4 M Fe/EDTA  
106 solution at a biogas flow rate of 265 mL min<sup>-1</sup> and at different liquid flow rates (22, 48,  
107 61, 70, 80, 122, 162, 207, 250 mL min<sup>-1</sup>). Despite the promising results obtained in terms  
108 of H<sub>2</sub>S removal, the use of Fe/EDTA solutions has been exclusively studied for H<sub>2</sub>S and  
109 NO<sub>x</sub> removal [14]. In this context, the performance of novel Fe/EDTA solutions enriched  
110 with carbonates must be tested in order to support a simultaneous removal of CO<sub>2</sub> and  
111 H<sub>2</sub>S from biogas at ambient pressure and temperature, which is expected to decrease both  
112 the investment and operating costs (the latter by one order of magnitude compared to  
113 conventional physical/chemical biogas upgrading technologies).

114

115 This study investigated, for the first time, the use of a chemical scrubbing process based  
116 on a Fe/EDTA/carbonate solution for the simultaneous removal of CO<sub>2</sub> and H<sub>2</sub>S from  
117 biogas in a single step process composed of a biogas absorption column interconnected  
118 to an air-aided regeneration column. A Taguchi L<sub>16</sub>(4<sup>5</sup>) experimental design was used in  
119 order to evaluate the influence of Fe/EDTA molarity, carbonate concentration, and  
120 biogas, air and liquid flow rates on biogas upgrading and to elucidate the optimal values  
121 of the parameters.

122

## 123 **2. Materials and methods**

### 124 **2.1 Biogas and Fe/EDTA solution**

125 The synthetic gas mixture used as a model biogas was composed of CH<sub>4</sub> (70%), CO<sub>2</sub>  
126 (29.5%) and H<sub>2</sub>S (0.5%) (Abello Linde; Spain). The Fe/EDTA/carbonate solution was  
127 prepared using iron (III) monosodium ethylenediaminetetraacetic (Alfa Aesar, Germany),  
128 sodium carbonate and sodium bicarbonate (Cofarcas, Spain).

129

## 130 **2.2 Experimental set-up**

131 The experimental lab scale set-up was located at the Institute of Sustainable Processes of  
132 Valladolid University (Spain). The lab scale set-up consisted of a biogas absorption  
133 column with a working volume of 1.8 L (internal diameter = 4 cm; height = 150 cm) and  
134 a regeneration column with a working volume of 2.0 L (internal diameter = 4 cm; height  
135 = 198 cm). Both columns were interconnected by a recirculation pump using a degassing  
136 chamber of 0.45 L (internal diameter = 8 cm; height = 9 cm). Biogas was injected in the  
137 absorption column under counter-current flow operation using a metallic diffuser of 2 μm  
138 pore size installed at the bottom of the column. Similarly, air was injected in the  
139 regeneration column under counter-current flow operation using a metallic diffuser of 2  
140 μm pore size installed at the bottom of the column (Fig. 1). The air and biogas flow rates  
141 were controlled via rotameter and mass flow controller, respectively (Aalborg, USA).

142

< **Figure 1** >

143

## 144 **2.3 Optimization of operational conditions by Taguchi's parameter design**

145 Five operational parameters (control factors) were selected in order to optimize the  
146 simultaneous removal of CO<sub>2</sub> and H<sub>2</sub>S from biogas, while preventing a negative O<sub>2</sub> and  
147 N<sub>2</sub> stripping from the scrubbing solution to biomethane: Fe/EDTA molarity (M),  
148 inorganic carbon concentration (IC), biogas flow rate (B), air flow rate (A) and  
149 recirculating liquid flow rate (L). M is an important factor determining the absorption of

150 H<sub>2</sub>S, while IC mediates the absorption of CO<sub>2</sub> from biogas. B, L and A were selected in  
151 order to study the influence of the recycling liquid/biogas ratio in the absorption column  
152 on biomethane quality and the efficiency of CO<sub>2</sub> desorption in the regeneration column.  
153 Four different levels were established for each control factor based on literature (Table  
154 1). The selection of such a high number of factor levels aimed at elucidating the behavior  
155 of the parameters within the tested range by identifying quadratic and sinusoidal effects  
156 [15]. The main objective of this work was the minimization of the concentration of CO<sub>2</sub>,  
157 H<sub>2</sub>S, O<sub>2</sub> and N<sub>2</sub> and the maximization of the concentration of CH<sub>4</sub> in the upgraded biogas.

158 **< Table 1 >**

159 The optimization of these five factors at the four different levels was carried out using a  
160 Taguchi's orthogonal array L<sub>16</sub>(4<sup>5</sup>) design [16]. The selected orthogonal array was a  
161 highly fractional factorial design that reduced the number of experiments from 4<sup>5</sup>=1024  
162 (required by a full factorial design) to 16, while still obtaining statistically meaningful  
163 results. The experimental design matrix resulted in a set of 16 experiments whose factor  
164 level combinations are depicted in Table 2. The order of execution of the 16 experiments  
165 was randomized and each test accounted for triplicate measurements of the upgraded  
166 biogas under steady state in order to be able to estimate the residual error of the analysis  
167 of variance (ANOVA). Each experiment lasted eight hours and a new solution was  
168 prepared for each replica. The pH value in each was set at 9.25 in order to allow an  
169 effective CO<sub>2</sub> and H<sub>2</sub>S capture from biogas at ambient pressure, while allowing a cost-  
170 effective air-aided CO<sub>2</sub> desorption. The investigation of the influence of pH on CO<sub>2</sub> and  
171 H<sub>2</sub>S removal was not necessary since its beneficial effect has been previously proved in  
172 many publications [17,18]. Mean results of the 16 experiments are shown in Table 2 and  
173 the results for each triplicate measurement are included in Table S1.

174 **< Table 2 >**

175 At this point it should be highlighted that the  $L_{16}(4^5)$  design has 15 degrees of freedom,  
176 (*d.f.*), which were all consumed by the use of five four-level control factors ( $5 \times (4-1) = 15$   
177 *d.f.*). No degrees of freedom were left to evaluate the interactions between control factors  
178 and therefore, interactions were integrated with the main effects according with the  
179 triangular interactions table of the design [19]. The  $L_{16}$  array was initially designed for  
180 two-level experiments. However, sets of mutually interactive columns of the  $L_{16}(2^{15})$   
181 array were merged to accommodate five four-level factors in order to use it for four-level  
182 experiments. The merging of mutually interactive columns minimized the above  
183 mentioned interactions [20].

184

185 The influence of the control factors on the performance of biogas upgrading was  
186 evaluated using ANOVA. The interactions between the most influential control factors,  
187 although integrated with the main effects, were graphically represented to evaluate their  
188 contribution. A Duncan's multiple range test was carried out in order to identify  
189 significant differences amongst factor levels and therefore to select those levels providing  
190 the optimum response during biogas upgrading [21].

191

192 All statistical calculations (ANOVA, Duncan's test and predictive models) were  
193 performed using Excel (Microsoft, USA).

194

#### 195 **2.4 Analytical procedures**

196 The concentrations of  $CH_4$ ,  $CO_2$ ,  $H_2S$ ,  $O_2$  and  $N_2$  in the biogas and biomethane were  
197 determined using a gas chromatograph coupled with a thermal conductivity detector  
198 (Varian CP-3800 GC-TCD, Palo Alto, USA) and equipped with a CP-Molsieve 5A (15  
199 m  $\times$  0.53 mm  $\times$  15  $\mu$ m) and a CP-PoraBOND Q (25 m  $\times$  0.53 mm  $\times$  15  $\mu$ m) columns.



200 The injector and detector temperatures were maintained at 150 and 175 °C, respectively.  
201 Helium was used as the carrier gas at 13.7 mL min<sup>-1</sup>. The pH was determined with an  
202 Eutech Cyberscan pH 510 (Eutech Instruments, The Netherlands). IC concentration was  
203 analyzed using a Shimadzu TOC-VCSH analyzer (Japan).

204

### 205 **3. Results and discussion**

#### 206 **3.1 Influence of the control factors on biogas upgrading**

207 The ANOVA of the experimental results (Table 3) demonstrated that the molarity of the  
208 Fe/EDTA solution was a significant factor influencing the concentration of all five biogas  
209 components according to the significance level used in all statistical calculations  
210 ( $p < 0.05$ ). The concentration of inorganic carbon in the solution directly impacted on the  
211 concentrations of CO<sub>2</sub>, N<sub>2</sub> and CH<sub>4</sub>, while the concentrations of CO<sub>2</sub>, O<sub>2</sub>, N<sub>2</sub> and CH<sub>4</sub>  
212 were affected by the biogas and recycling liquid flow rates. Finally, the air flow rate in  
213 the stripping column also influenced the CO<sub>2</sub>, H<sub>2</sub>S, N<sub>2</sub> and CH<sub>4</sub> content.

214

#### **<Table 3>**

215 The effect of each factor level on the mean values of the concentration of the target  
216 components in the upgraded biogas is shown in Fig. 2. The CO<sub>2</sub> concentration values  
217 obtained at the four different levels of M (0, 0.01, 0.03, 0.05) were 4.3, 6.9, 5.6 and 16.1%,  
218 respectively. At this point, it is important to stress that this increase in CO<sub>2</sub> concentration  
219 recorded at the highest molarity was not likely influenced by the increase in the molarity  
220 of the Fe/EDTA solution but related to the interactions of the different levels of each  
221 control factor assessed in the test at 0.05 M of Fe/EDTA. A decrease in CO<sub>2</sub> concentration  
222 was observed at increasing inorganic carbon concentration, from 13.1% at 4000 mg IC L<sup>-1</sup>  
223 to 4.5% at 10000 mg IC L<sup>-1</sup>. The pH values recorded in each experiment in the  
224 absorption column are collected in Table S2. A higher inorganic carbon concentration in

225 the absorption solution entailed a higher pH and buffer capacity, which provided an  
226 enhanced transfer of CO<sub>2</sub>. The increase in biogas flow rate brought about an increase in  
227 CO<sub>2</sub> concentration of the upgraded biogas, from 2.5% at 10 mL min<sup>-1</sup> to 13.8% at 40 mL  
228 min<sup>-1</sup>, as a result of the corresponding reduction in the biogas residence time in the  
229 absorption column. Air flow rates of 200, 500 and 1000 mL min<sup>-1</sup> in the desorption  
230 column supported CO<sub>2</sub> concentrations of 7.5, 8.0 and 6.7%, respectively, while a higher  
231 CO<sub>2</sub> concentration value of 10.8% was recorded at 800 mL min<sup>-1</sup>. Finally, CO<sub>2</sub>  
232 concentrations of 8.3 and 7.9% were achieved at recycling liquid flow rates of 5 and 20  
233 mL min<sup>-1</sup>, respectively; while a higher CO<sub>2</sub> concentration of 10.9% was recorded at 10  
234 mL min<sup>-1</sup>. A liquid flow rate of 30 mL min<sup>-1</sup> provided a CO<sub>2</sub> concentration of 5.9% (Fig.  
235 2a).

236 **<Figure 2>**

237 A decrease in H<sub>2</sub>S concentration was observed as the Fe/EDTA molarity increased, from  
238 0.035% at 0.00 M to 0.000% at a concentration of 0.05 M. These results can be explained  
239 by the capacity of the Fe/EDTA solution to partially oxidize the H<sub>2</sub>S present in biogas.  
240 No clear correlation between the H<sub>2</sub>S concentration and the air flow rate in the upgraded  
241 biogas was observed, with values of 0.021, 0.014, 0.024 and 0.011% at air flow rates of  
242 200, 500, 800 and 1000 mL min<sup>-1</sup>, respectively (Fig. 2b). The IC concentration, biogas  
243 and liquid flow rates did not exert a significant effect on the elimination of H<sub>2</sub>S according  
244 to the statistical analysis at p>0.05 (Table 3). The increase in biogas flow rate induced a  
245 slight decrease in H<sub>2</sub>S levels, which suggests the interference of other factors since a  
246 decrease in biogas residence time in the absorption column should entail a reduction in  
247 H<sub>2</sub>S removal efficiencies.

248

249 O<sub>2</sub> concentrations of 0.25, 0.14, 0.25 and 0.18% were recorded at Fe/EDTA molarities of  
250 0.00, 0.01, 0.03 and 0.05 M, respectively. A decrease in O<sub>2</sub> concentration was observed  
251 at increasing biogas flow rates, from 0.34% at 10 mL min<sup>-1</sup> to 0.16% at 40 mL min<sup>-1</sup>, as  
252 a result of the enhanced dilution of the stripped oxygen. Finally, the decrease in O<sub>2</sub>  
253 concentration at increasing liquid flow rates, from 0.24% at a flow rate of 5 mL min<sup>-1</sup> to  
254 0.15% at a flow rate of 30 mL min<sup>-1</sup>, suggests the interference of other factors, since a  
255 higher recycling liquid flow rate should entail a higher O<sub>2</sub> stripping (Fig. 2c). The IC  
256 concentration and air flow rate did not exert a significant effect on O<sub>2</sub> content (ANOVA  
257 test at p>0.05, Table 3).

258

259 Although all the parameters significantly influenced the elimination of N<sub>2</sub> (p < 0.05,  
260 Table 3), no clear correlations between N<sub>2</sub> concentration in the upgraded biogas and the  
261 experimental parameters were observed. The N<sub>2</sub> concentrations recorded at a Fe/EDTA  
262 molarity of 0.00, 0.01, 0.03 and 0.05 M were 1.00, 0.87, 0.58 and 0.80%, respectively.  
263 N<sub>2</sub> concentrations of 0.84, 0.62, 0.96 and 0.83% were recorded at IC concentrations of  
264 4000, 6000, 8000 and 10000 mg L<sup>-1</sup>, respectively. Similarly, N<sub>2</sub> concentrations of 1.28,  
265 0.54, 0.77 and 0.65% were achieved at biogas flow rates of 10, 20, 30 and 40 mL min<sup>-1</sup>,  
266 respectively, and of 0.84, 0.61, 1.00 and 0.79% at air flow rates of 200, 500, 800 and 1000  
267 mL min<sup>-1</sup>, respectively. Finally, recycling liquid flow rates of 5, 10, 20 and 30 mL min<sup>-1</sup>  
268 supported N<sub>2</sub> concentrations of 0.95, 0.72, 0.91 and 0.67%, respectively (Fig 2d).

269

270 CH<sub>4</sub> concentrations in the upgraded biogas at Fe/EDTA molarities of 0.00, 0.01, 0.03 and  
271 0.05 M were 94.4, 92.0, 93.5 and 82.9%, respectively. It is important to stress that the  
272 decrease in CH<sub>4</sub> concentration recorded at 0.05 M of Fe/EDTA was due to the high CO<sub>2</sub>  
273 concentration in the upgraded biogas likely caused by the interactions of the different

274 levels of each control factor assessed in the tests at 0.05 M of Fe/EDTA. An increase in  
275 CH<sub>4</sub> concentration was observed at increasing IC concentrations, from 85.9% at 4000 mg  
276 IC L<sup>-1</sup> to 94.5% at 10000 mg IC L<sup>-1</sup>. The increase in biogas flow rate mediated a decrease  
277 in the CH<sub>4</sub> concentration of the upgraded biogas, from 95.9% at 10 mL min<sup>-1</sup> to 85.4% at  
278 40 mL min<sup>-1</sup>. On the other hand, air flow rates of 200, 500 and 1000 mL min<sup>-1</sup> in the  
279 stripping column supported CH<sub>4</sub> concentrations of 91.5, 91.2 and 92.2%, respectively,  
280 while a lower CH<sub>4</sub> concentration of 87.9% was observed at 800 mL min<sup>-1</sup> when the  
281 medium contained the lowest IC concentration. Finally, recycling liquid flow rates of 5,  
282 10, 20 and 30 mL min<sup>-1</sup> corresponded to CH<sub>4</sub> concentrations of 90.5, 88.1, 91.0 and  
283 93.3%, respectively (Fig. 2e).

284

285 In the particular case of CO<sub>2</sub>, N<sub>2</sub> and CH<sub>4</sub> concentrations, the five control factors tested  
286 were decisive in order to fulfill any biomethane standard. The Fe/EDTA molarity and air  
287 flow rate were significant to minimize H<sub>2</sub>S concentration, while the most relevant factors  
288 determining the O<sub>2</sub> concentration in the upgraded biogas were the liquid and biogas flow  
289 rates and the Fe/EDTA molarity.

290

### 291 **3.2 Process optimization**

292 A Duncan's multiple range test was performed in order to verify the optimal level for  
293 each control factor and to obtain the operational conditions optimizing the upgrading of  
294 biogas. The test was applied to the factors with a significant effect on the concentration  
295 of the different gases measured in the upgraded biogas. According to the test results, the  
296 combination of levels of each control factor that minimized the concentration of CO<sub>2</sub>,  
297 H<sub>2</sub>S, O<sub>2</sub> and N<sub>2</sub> in the upgraded biogas and maximized the concentration of CH<sub>4</sub> was

298 M<sub>4</sub>-IC<sub>1</sub>-B<sub>2</sub>-A<sub>4</sub>-L<sub>4</sub>, which corresponds to 0.03 M Fe/EDTA, 10000 mg IC L<sup>-1</sup>, 10 mL min<sup>-1</sup>  
299 <sup>1</sup> of biogas flow rate, 1000 mL min<sup>-1</sup> of air flow rate and 30 mL min<sup>-1</sup> of liquid flow rate.

300

301 A visual analysis of the interaction between Fe/EDTA molarity and the inorganic carbon  
302 concentration was also performed by jointly representing the mean responses obtained  
303 for CO<sub>2</sub> and H<sub>2</sub>S at the tested levels of Fe/EDTA molarity and IC (Fig. 3). According to  
304 this analysis, a change in Fe/EDTA molarity from 0.03 M to 0.05 entailed an increase in  
305 CO<sub>2</sub> concentration above 15% for IC levels ranging from 4000 to 8000 mg L<sup>-1</sup>, but the  
306 impact is negligible if the maximum 10000 mg L<sup>-1</sup> IC level is used, at which CO<sub>2</sub>  
307 concentration is around 5% independently of the Fe/EDTA concentration. On the other  
308 hand, a change in Fe/EDTA molarity from 0.03 to 0.05 M corresponded to changes in  
309 H<sub>2</sub>S concentrations from 0.023, 0.006, 0.016 and 0.014% (at IC concentrations of 4000,  
310 6000, 8000 and 10000 mg L<sup>-1</sup>, respectively) to 0.000% regardless of the IC concentration  
311 level (Fig. 3b). Therefore, the optimum combination resulting from the Duncan's multiple  
312 range test (M<sub>4</sub>-IC<sub>1</sub>-B<sub>2</sub>-A<sub>4</sub>-L<sub>4</sub>) can be changed to the optimum combination resulting  
313 from the analysis of interactions, M<sub>2</sub>-IC<sub>1</sub>-B<sub>2</sub>-A<sub>4</sub>-L<sub>4</sub>: 0.05 M Fe/EDTA - 10000 mg L<sup>-1</sup>  
314 IC- 10 mL min<sup>-1</sup> biogas - 1000 mL min<sup>-1</sup> air - 30 mL min<sup>-1</sup> liquid.

315

### <Figure 3>

316 The model equations for each design response, calculated with Excel using multiple linear  
317 regression (MLR) [22], can be represented by equations (9) to (13). The confidence  
318 intervals of the coefficients were calculated as the product of the standard deviation of  
319 the coefficient and the student-t statistic for 0.05 significance level and n - k degrees of  
320 freedom, where *n* is the number of experiments (16) and *k* the number of model coefficients  
321 (6).

$$322 \text{CO}_2 (\%) = 8.25 + 2.57M - 2.09IC + 2.75B + 0.13A - 0.86L \quad (9)$$

323  $R^2 = 81.0\%$

324  $H_2S (\%) = 0.0175 - 0.0079M - 0.0006IC - 0.0026B - 0.0014A + 0.0009L$  (10)

325  $R^2 = 77.8\%$

326  $O_2 (\%) = 0.205 - 0.003M - 0.007IC - 0.043B + 0.015A - 0.024L$  (11)

327  $R^2 = 53.6\%$

328  $N_2 (\%) = 0.811 - 0.060M + 0.023IC - 0.123B + 0.023A - 0.043L$  (12)

329  $R^2 = 32.3\%$

330  $CH_4 (\%) = 90.72 - 2.50M + 2.08IC - 2.58B - 0.17A - 0.93L$  (13)

331  $R^2 = 79.1\%$

332 where  $R^2$  is the coefficient of determination. Low  $R^2$  values may result from uncontrolled  
333 influencing factors (noise factors) or unconsidered quadratic interactions or effects. The  
334 biomethane composition predicted by the model under the operational conditions  
335 optimized according to the analysis of the effect of interactions ( $M_2$ - $IC_1$ - $B_2$ - $A_4$ - $L_4$ ) was:  
336  $CO_2 = 2.6\%$ ,  $H_2S = 0.004\%$ ,  $O_2 = 0.25\%$ ,  $N_2 = 0.92\%$  and  $CH_4 = 96.3\%$ . These values  
337 comply with the requirements of most international biomethane standards ( $CH_4 \geq 90$ -  
338  $95\%$ ,  $CO_2 \leq 2$ - $4\%$ ,  $O_2 \leq 1\%$  and negligible amounts of  $H_2S$ ) [2,5,6].

339

340 Models with interactions and quadratic terms can be described by equations S1 to S5,  
341 which have been included in the supplementary material document, seem to fit better to  
342 the experimental data derived from the design of experiments (improving the coefficient  
343 of determination). However, the prediction of the concentration of  $CO_2$ ,  $H_2S$  and  $CH_4$   
344 ( $7.0\%$ ,  $0.000\%$  and  $92.1\%$ , respectively) derived from these models for the experiment  
345 performed under the selected optimal conditions did not match the results obtained  
346 experimentally. The prediction from the models that only included the main effects was

347 much closer to the experimental results, which ultimately supported the use of linear  
348 regression instead of quadratic interactions.

349

### 350 **3.3 Continuous biogas upgrading operation**

351 The optimal combinations of factor levels identified in the Duncan's multiple range test  
352 and in the analysis of the effect of interaction  $M \times IC$  were not tested in any of the 16  
353 experiments of the Taguchi's  $L_{16}(4^5)$  orthogonal array. Thus, both combinations were  
354 subsequently tested under continuous operation in order to confirm the expected results  
355 and to evaluate the stability of the process over time. The optimum Duncan test  
356 combination  $M_4-IC_1-B_2-A_4-L_4$  (0.03 M - 10000 mg L<sup>-1</sup> - 10 mL min<sup>-1</sup> - 1000 mL min<sup>-1</sup> -  
357 30 mL min<sup>-1</sup>) was tested from days 0 to 9, and the optimum combination derived from  
358 the analysis of the effect of interaction  $M \times IC$  ( $M_2-IC_1-B_2-A_4-L_4$ : 0.05 M - 10000 mg  
359 L<sup>-1</sup> - 10 mL min<sup>-1</sup> - 1000 mL min<sup>-1</sup> - 30 mL min<sup>-1</sup>) was tested from days 9 to 19.

360

361 The CO<sub>2</sub> concentration in the biomethane using the optimum Duncan's test combination  
362 (stage I) was  $1.5 \pm 0.3\%$ , corresponding to CO<sub>2</sub> removal efficiencies (REs) of 95.1%.  
363 Biogas upgrading under the optimum combination from the analysis of the effect of  
364 interactions (stage II) entailed a CO<sub>2</sub> concentration of  $1.4 \pm 0.2\%$ , which corresponded to  
365 CO<sub>2</sub>-REs of 95.5% (Fig. 4a). These CO<sub>2</sub>-REs were higher than those previously reported  
366 by Horikawa et al., [11], who recorded CO<sub>2</sub>-REs ranging from 4.0% to 16.0% using an  
367 aqueous solution of 0.2 M Fe/EDTA in a system composed of an absorption and a  
368 regeneration column with a total volume of 0.82 L, and operated with a biogas flow rate  
369 of 1000 mL min<sup>-1</sup> and a liquid flow rate of 83 mL min<sup>-1</sup>. CO<sub>2</sub> absorption at industrial  
370 scale can be increased by operating at a high pH value in the scrubbing solution and by  
371 increasing the liquid to biogas ratio without compromising O<sub>2</sub> and N<sub>2</sub> levels in

372 biomethane. The former would increase the gas-liquid concentration gradient in the  
373 biogas absorption column, while the latter would increase both the overall mass transfer  
374 coefficient between the liquid and the biogas and the total absorption capacity of the  
375 column.

376

377 H<sub>2</sub>S concentration during stage I was  $0.013 \pm 0.004\%$ , corresponding to H<sub>2</sub>S-REs of  
378 96.8%, while the increase in Fe/EDTA concentration from 0.03 to 0.05 M applied in stage  
379 II resulted in a complete removal of H<sub>2</sub>S from biogas (Fig. 4b). These results confirmed  
380 that the analysis of the effect of interactions provided the best combination of operational  
381 parameters due to its capacity to completely remove H<sub>2</sub>S from biogas. These results were  
382 superior than those previously reported by Horikawa et al., [11], who recorded H<sub>2</sub>S-REs  
383 of 90.0% in a similar experimental set-up operated at 0.2 M Fe/EDTA, a biogas flow rate  
384 of  $1000 \text{ mL min}^{-1}$  and a liquid flow rate of  $83 \text{ mL min}^{-1}$ . Likewise, Schiavon Maia et al.,  
385 [12] reported H<sub>2</sub>S-REs of 91.4% in a similar system configuration operated at 0.2 M  
386 Fe/EDTA, with biogas and liquid flow rates of  $340 \text{ mL min}^{-1}$ .

387

388 The O<sub>2</sub> concentration in the upgraded biogas remained roughly constant in both stages,  
389 the recorded values being  $0.37 \pm 0.11\%$  and  $0.29 \pm 0.03\%$  for stages I and II, respectively  
390 (Fig. 4c). On the other hand, the N<sub>2</sub> concentration recorded during stage I was  $1.17 \pm$   
391  $0.24\%$  and  $0.97 \pm 0.08\%$  during stage II (Fig. 4d).

392

393 Finally, CH<sub>4</sub> concentrations in the upgraded biogas of  $97.0 \pm 0.3\%$  in stage I and  $97.4 \pm$   
394  $0.2\%$  in stage II were achieved (Fig. 4e). These high CH<sub>4</sub> concentration values together  
395 with the high CO<sub>2</sub>-REs and H<sub>2</sub>S-REs confirmed that this innovative technology  
396 represents a superior option for the upgrading of biogas compared with conventional



397 biological or physicochemical technologies. These results confirmed that the use of this  
398 single step technology at ambient temperature and pressure, and without continuous  
399 chemical addition, was feasible since the biomethane obtained during stage I and II  
400 complied with the European Biomethane Standard EN 16723 for injection into natural  
401 gas grids or use as a vehicle fuel ( $\text{CH}_4 \geq 90\text{-}95\%$ ,  $\text{CO}_2 \leq 2\text{-}4\%$  and  $\text{O}_2 \leq 1\%$ ) [2,5,6]. A  
402 siloxane and water removal would be however required to fulfill the above mentioned  
403 biomethane Standard. The results also confirmed the values predicted by the model  
404 equations resulting from the experimental design and support the use of fractional  
405 factorial experimental designs in optimization of multifactor processes.

406 **<Figure 4>**

407 Despite a new chemical solution was prepared for each replica when assessing the  
408 upgrading capacity of each series of operational conditions, the Fe/EDTA/carbonate  
409 solution herein proposed can be used during long operational periods. Thus, the absorbed  
410  $\text{CO}_2$  decreases the pH of the scrubbing solution, which is further restored as a result of  
411 the air-aided  $\text{CO}_2$  stripping. Similarly,  $\text{H}_2\text{S}$  is oxidized using  $\text{Fe}^{3+}$  following equation 6,  
412 and the resulting  $\text{Fe}^{2+}$  is regenerated in the stripping column according to equation 8.

413

414 The main limitation encountered during the continuous operation of this technology was  
415 foam formation in the regeneration column due to the high air flow rate used ( $1000 \text{ mL}$   
416  $\text{min}^{-1}$ ). To overcome this problem, 10.0 mL of antifoam 204 (Sigma-Aldrich, USA) were  
417 added on day 6 and 2.0 mL were added on days 7, 8 and 13. For the design of the  
418 absorption and stripping columns at industrial scale it is important to consider the fact  
419 that the air flow required in the regeneration column is significantly higher than the biogas  
420 flow pumped into the absorption column. This results in the need of larger regeneration  
421 columns compared to the absorption column. The sulphur produced from  $\text{H}_2\text{S}$  oxidation

422 throughout the continuous operation was easily recoverable from the bottom of both  
423 columns at the end of the process.

424

### 425 **3.4 Energy study**

426 An energy analysis was conducted in order to obtain the power consumption of this  
427 technology for the upgrading of 300 Nm<sup>3</sup> h<sup>-1</sup> of biogas. Power consumption for biogas  
428 sparging in the absorption column and air sparging in the regeneration column were  
429 calculated according to Eq. (14), and the power required for liquid recirculation between  
430 both columns was calculated according to Eq. (15).

$$431 \quad E_{gas} = \frac{Q_{gas} \times \Delta P}{0.7} \quad (14)$$

$$432 \quad E_{liq} = \frac{Q_{liq} \times \rho \times g \times H}{0.7} \quad (15)$$

433 where  $Q_{gas}$  is the flowrate of biogas or air (m<sup>3</sup> s<sup>-1</sup>),  $\Delta P$  is the pressure drop (kPa),  $Q_{liq}$  is  
434 the flowrate of liquid between both columns (m<sup>3</sup> s<sup>-1</sup>),  $H$  is water column height (m),  $\rho$  is  
435 the water density (kg m<sup>-3</sup>),  $g$  is the Earth gravity constant (m s<sup>-2</sup>).

436

437 The electricity demand of the system accounted for 0.02 kW-h (Nm<sup>3</sup>)<sup>-1</sup> of biogas treated.  
438 This low value of the Fe/EDTA/carbonate-based scrubbing process compare positively  
439 with the 0.2 – 0.3 kW-h (Nm<sup>3</sup>)<sup>-1</sup> of biogas treated of conventional processes such as water  
440 or organic solvent scrubbing, pressure swing adsorption and membrane separation.

441

## 442 **4. Conclusions**

443 This study demonstrated the effectiveness and stability of Fe/EDTA/carbonate-based  
444 scrubbing for the simultaneous removal of H<sub>2</sub>S and CO<sub>2</sub> from biogas. This innovative  
445 process was able to operate at ambient pressure and temperature, and without external  
446 chemical addition, which supported an energy demand 10 times lower than their

447 physical/chemical counterparts. The experimental Taguchi's design revealed the  
448 significant influence of Fe/EDTA molarity, inorganic carbon concentration, biogas flow  
449 rate, air flow rate and recirculating liquid flow rate on biomethane quality. An effective  
450 optimization via a Duncan's multiple range test and an analysis of the effect of  
451 interactions provided the optimal conditions for each control factor in order to maximize  
452 the CH<sub>4</sub> content and minimize CO<sub>2</sub>, O<sub>2</sub>, N<sub>2</sub> and H<sub>2</sub>S content in biomethane. Continuous  
453 biogas upgrading in this innovative absorption-stripping system at 0.05 Fe/EDTA, 10000  
454 mg IC L<sup>-1</sup>, 10 mL biogas min<sup>-1</sup>, 1000 mL air min<sup>-1</sup> and 30 mL liquid min<sup>-1</sup> supported  
455 concentrations of CH<sub>4</sub> > 97%, CO<sub>2</sub> < 2% and O<sub>2</sub> < 1%, which complied with most  
456 international biomethane regulations.

457

#### 458 **Acknowledgements**

459 This work was supported by the Regional Government of Castilla y León and the EU-  
460 FEDER programme (CLU 2017-09 and UIC 071). The financial support of the Regional  
461 Government of Castilla y León is also acknowledged for the PhD grant of David Marín.

462

#### 463 **REFERENCES**

- 464 [1] D. Andriani, A. Wresta, T.D. Atmaja, A. Saepudin, A review on optimization  
465 production and upgrading biogas through CO<sub>2</sub> removal using various techniques,  
466 Appl. Biochem. Biotechnol. 172 (2014) 1909–1928. [https://doi.org/10.1007/s12010-](https://doi.org/10.1007/s12010-013-0652-x)  
467 013-0652-x.
- 468 [2] R. Muñoz, L. Meier, I. Diaz, D. Jeison, A review on the state-of-the-art of  
469 physical/chemical and biological technologies for biogas upgrading, Rev. Environ.  
470 Sci. Bio/Technology. 14 (2015) 727–759. [https://doi.org/10.1007/s11157-015-9379-](https://doi.org/10.1007/s11157-015-9379-1)  
471 1.

- 472 [3] European Biogas Association, EBA Statistical Report 2018, (2018).  
473 <https://www.europeanbiogas.eu/eba-statistical-report-2018/> (accessed December 2,  
474 2019).
- 475 [4] E. Ryckebosch, M. Drouillon, H. Vervaeren, Techniques for transformation of biogas  
476 to biomethane, *Biomass and Bioenergy*. 35 (2011) 1633–1645.  
477 <https://doi.org/10.1016/j.biombioe.2011.02.033>.
- 478 [5] European Committee for Standardization, UNE EN 16723-2:2018 Natural gas and  
479 biomethane for use in transport and biomethane for injection in the natural gas network  
480 - Part 2: Automotive fuels specification, (2018). [https://www.en-standard.eu/une-en-  
481 16723-2-2018-natural-gas-and-biomethane-for-use-in-transport-and-biomethane-for-  
482 injection-in-the-natural-gas-network-part-2-automotive-fuels-specification/](https://www.en-standard.eu/une-en-16723-2-2018-natural-gas-and-biomethane-for-use-in-transport-and-biomethane-for-injection-in-the-natural-gas-network-part-2-automotive-fuels-specification/) (accessed  
483 December 10, 2019).
- 484 [6] European Committee for Standardization, UNE EN 16723-1:2017 Natural gas and  
485 biomethane for use in transport and biomethane for injection in the natural gas network  
486 - Part 1: Specifications for biomethane for injection in the natural gas network, (2017).  
487 [https://www.en-standard.eu/une-en-16723-1-2017-natural-gas-and-biomethane-for-  
488 use-in-transport-and-biomethane-for-injection-in-the-natural-gas-network-part-1-  
489 specifications-for-biomethane-for-injection-in-the-natural-gas-network/](https://www.en-standard.eu/une-en-16723-1-2017-natural-gas-and-biomethane-for-use-in-transport-and-biomethane-for-injection-in-the-natural-gas-network-part-1-specifications-for-biomethane-for-injection-in-the-natural-gas-network/) (accessed  
490 December 10, 2019).
- 491 [7] I. Angelidaki, L. Treu, P. Tsapekos, G. Luo, S. Campanaro, H. Wenzel, P.G. Kougias,  
492 Biogas upgrading and utilization: current status and perspectives, *Biotechnol. Adv.* 36  
493 (2018) 452–466. <https://doi.org/10.1016/j.biotechadv.2018.01.011>.
- 494 [8] B. Stürmer, F. Kirchmeyr, K. Kovacs, F.H. Gba, D.C. Rea, I. Atee, J.S. Eba, S. Proietti,  
495 Technical-economic analysis for determining the feasibility threshold for tradable

496 biomethane certificates, (2016) 1–24. [http://www.ergar.org/wp-](http://www.ergar.org/wp-content/uploads/2018/07/BIOSURF-D3.4.pdf)  
497 [content/uploads/2018/07/BIOSURF-D3.4.pdf](http://www.ergar.org/wp-content/uploads/2018/07/BIOSURF-D3.4.pdf) (accessed June 1, 2020).

498 [9] O.W. Awe, Y. Zhao, A. Nzihou, D.P. Minh, N. Lyczko, A review of biogas utilisation,  
499 purification and upgrading technologies, *Waste and Biomass Valorization*. 8 (2017)  
500 267–283. <https://doi.org/10.1007/s12649-016-9826-4>.

501 [10] H.J. Wubs, A.A.C.M. Beenackers, Kinetics of H<sub>2</sub>S absorption into aqueous ferric  
502 solutions of edta and hedta, *Ind. Eng. Chem. Res.* 32 (1993) 2580–2594.  
503 <https://doi.org/10.1021/ie00023a022>.

504 [11] M.S. Horikawa, F. Rossi, M.L. Gimenes, C.M.M. Costa, M.G.C. Da Silva,  
505 Chemical absorption of H<sub>2</sub>S for biogas purification, *Brazilian J. Chem. Eng.* 21 (2004)  
506 415–422. <https://doi.org/10.1590/S0104-66322004000300006>.

507 [12] D.C. Schiavon Maia, R.R. Niklevicz, R. Arioli, L.M. Frare, P.A. Arroyo, M.L.  
508 Gimenes, N.C. Pereira, Removal of H<sub>2</sub>S and CO<sub>2</sub> from biogas in bench scale and the  
509 pilot scale using a regenerable Fe-EDTA solution, *Renew. Energy*. 109 (2017) 188–  
510 194. <https://doi.org/10.1016/j.renene.2017.03.023>.

511 [13] L.M. Frare, M.G.A. Vieira, M.G.C. Silva, N.C. Pereira, M.L. Gimenes, Hydrogen  
512 sulfide removal from biogas using Fe/EDTA solution: Gas/Liquid contacting and  
513 sulfur formation, *Environ. Prog. Sustain. Energy*. 29 (2010).  
514 <https://doi.org/10.1002/ep>.

515 [14] W. Li, J. Zhao, L. Zhang, Y. Xia, N. Liu, S. Li, S. Zhang, Pathway of FeEDTA  
516 transformation and its impact on performance of NO<sub>x</sub> removal in a chemical  
517 absorption-biological reduction integrated process, *Sci. Rep.* 6 (2016) 18876.  
518 <https://doi.org/10.1038/srep18876>.

519 [15] R. Roy, Design of experiments using the Taguchi approach: 16 steps to product  
520 and process improvement, John Wiley & Sons, New York, USA, 2001, p. 560.

- 521 [16] G. Taguchi, S. Chowdhury, Y. Wu, Taguchi's quality engineering handbook, John  
522 Wiley & Sons, New York, USA, 2004, p. 1696.
- 523 [17] E. Tilahun, E. Sahinkaya, B. Çalli, Effect of operating conditions on separation of  
524 H<sub>2</sub>S from biogas using a chemical assisted PDMS membrane process, Waste and  
525 Biomass Valorization. 9 (2018) 2349–2359. [https://doi.org/10.1007/s12649-018-](https://doi.org/10.1007/s12649-018-0226-9)  
526 0226-9.
- 527 [18] E. Tilahun, E. Sahinkaya, B. Çalli, A hybrid membrane gas absorption and  
528 biooxidation process for the removal of hydrogen sulfide from biogas, Int. Biodeterior.  
529 Biodegradation. 127 (2018) 69–76.  
530 [https://doi.org/https://doi.org/10.1016/j.ibiod.2017.11.015](https://doi.org/10.1016/j.ibiod.2017.11.015).
- 531 [19] N. Logothetis, H.P. Wynn, Quality through design: experimental design, off-line  
532 quality control, and Taguchi's contributions, Oxford University Press, Michigan,  
533 USA, 1994, p. 464.
- 534 [20] S.H. Park, J. Antony, Robust design for quality engineering and six sigma, in:  
535 World Scientific, Danvers, USA, 2008, p. 545.
- 536 [21] P.J. Ross, Taguchi techniques for quality engineering: loss function, orthogonal  
537 experiments, parameter and tolerance design, McGraw-Hill, New York, USA, 1988,  
538 p. 329.
- 539 [22] B.G.M. Vandeginste, D.L. Massart, L.M.C. Buydens, S. De Jong, P.J. Lewi, J.  
540 Smeyers-Verbeke, Handbook of chemometrics and qualimetrics: Part B, Elsevier  
541 Science, Amsterdam, The Netherlands, 1998, p. 867.

542

543 **FIGURE CAPTIONS**

544 **Figure 1.** Schematic diagram of the experimental plant used for the integral upgrading of  
545 biogas.

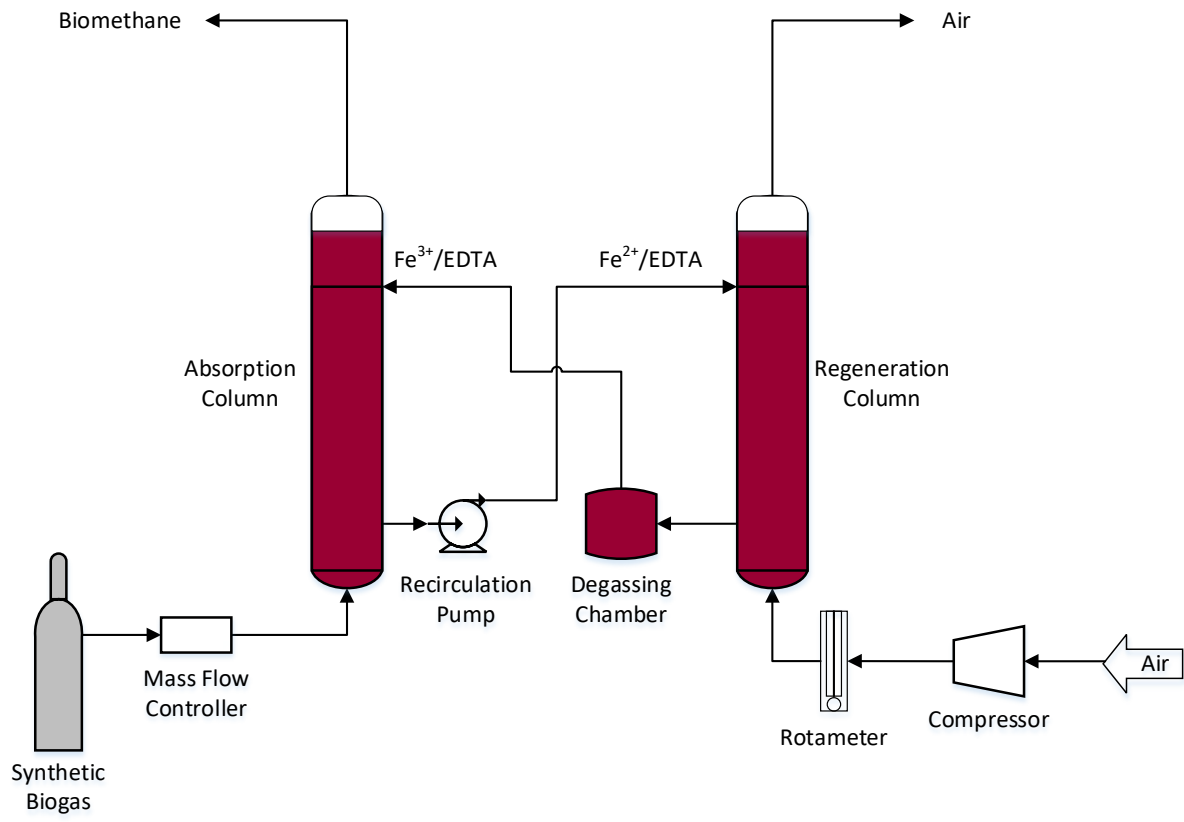
546 **Figure 2.** Influence of the control factors on the mean response of (a) CO<sub>2</sub> (■), (b) H<sub>2</sub>S  
547 (●), (c) O<sub>2</sub> (▲), (d) N<sub>2</sub> (□) and (e) CH<sub>4</sub> (○) concentration in the upgraded biogas.

548 **Figure 3.** Effect of interactions between Fe/EDTA molarity and inorganic carbon  
549 concentration ((■) 4000, (○) 6000, (▲) 8000 and (◇) 10000 mg L<sup>-1</sup>) on the  
550 concentrations of (a) CO<sub>2</sub> and (b) H<sub>2</sub>S in the upgraded biogas.

551 **Figure 4.** Time course of the concentration of (a) CO<sub>2</sub> (■), (b) H<sub>2</sub>S (●), (c) O<sub>2</sub> (▲), (d)  
552 N<sub>2</sub> (□) and (e) CH<sub>4</sub> (○) in the upgraded biogas.

553

554 **Figure 1.** Schematic diagram of the experimental plant used for the integral upgrading  
555 of biogas.

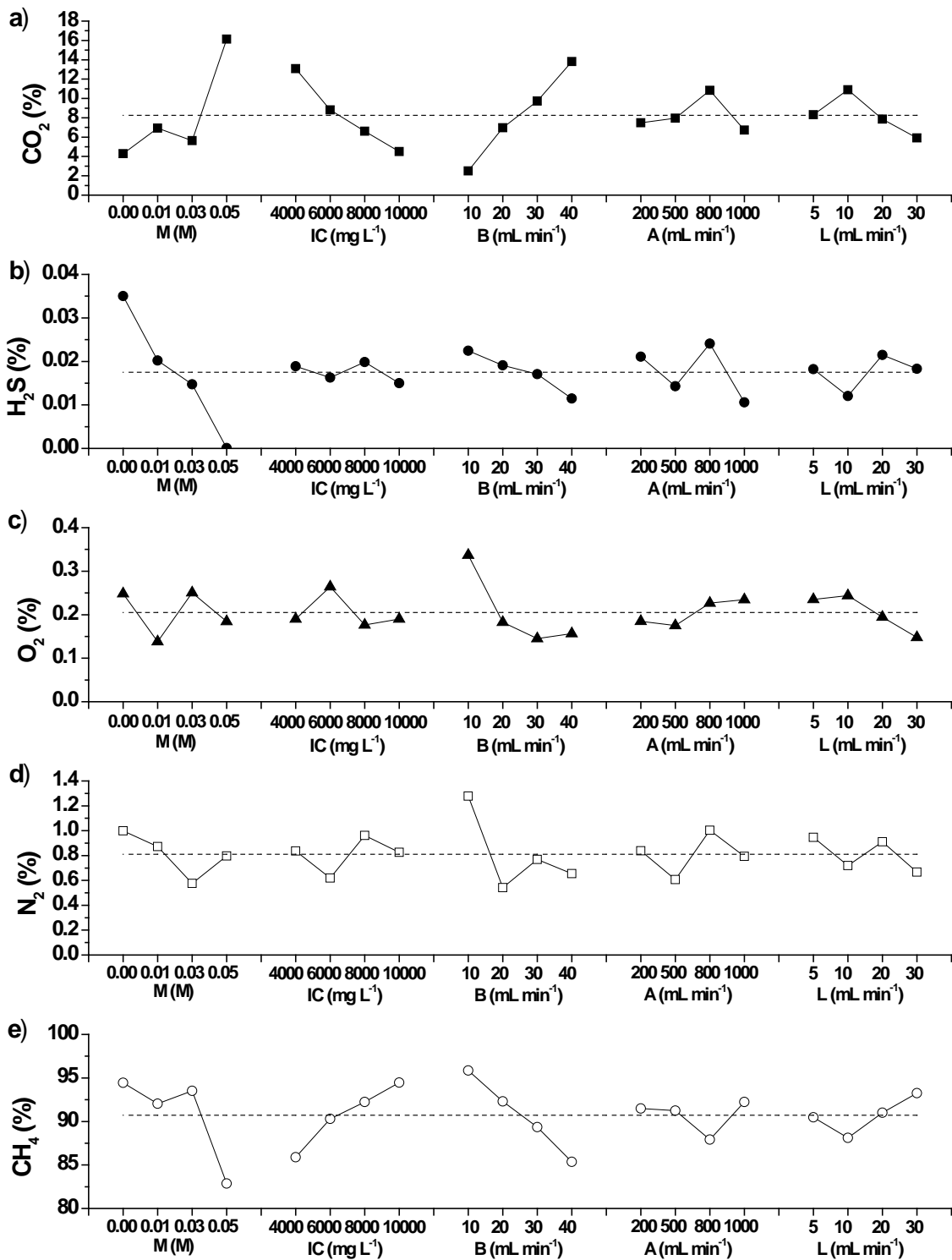


556

557



558 **Figure 2.** Influence of the control factors on the mean response of (a) CO<sub>2</sub> (■), (b) H<sub>2</sub>S  
 559 (●), (c) O<sub>2</sub> (▲), (d) N<sub>2</sub> (□) and (e) CH<sub>4</sub> (○) concentration in the upgraded biogas.



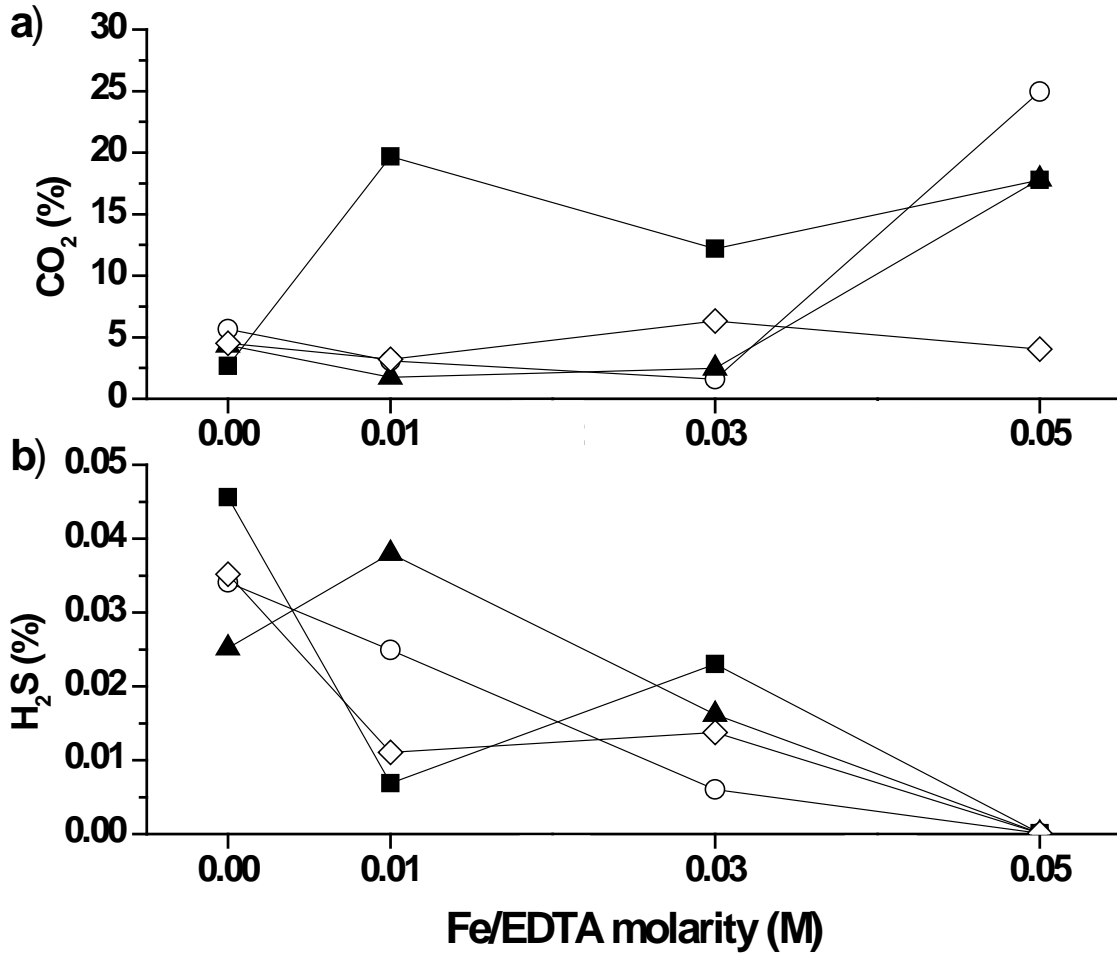
560

561

562 **Figure 3.** Effect of interactions between Fe/EDTA molarity and inorganic carbon

563 concentration ((■) 4000, (○) 6000, (▲) 8000 and (◇) 10000 mg L<sup>-1</sup>) on the

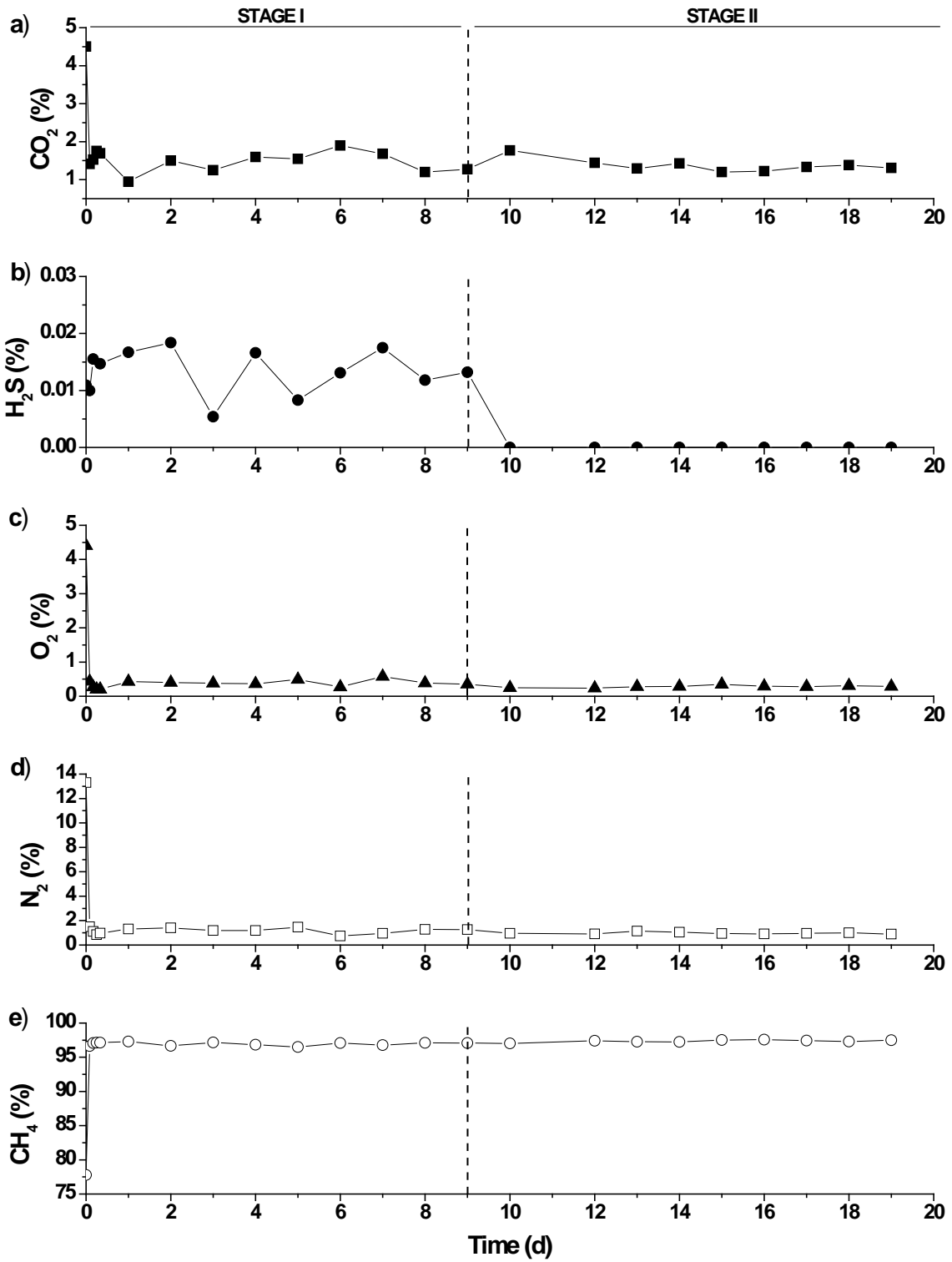
564 concentrations of (a) CO<sub>2</sub> and (b) H<sub>2</sub>S in the upgraded biogas.



565

566

567 **Figure 4.** Time course of the concentration of (a) CO<sub>2</sub> (■), (b) H<sub>2</sub>S (●), (c) O<sub>2</sub> (▲), (d)  
 568 N<sub>2</sub> (□) and (e) CH<sub>4</sub> (○) in the upgraded biogas.



569

570

571

**Table 1.** Factors and levels for the optimization of biogas upgrading

Factor	Acronym	Levels			
		1	2	3	4
Fe/EDTA Molarity (M)	M	0.00	0.05	0.01	0.03
Inorganic Carbon Concentration (mg L <sup>-1</sup> )	IC	10000	4000	6000	8000
Biogas Flow rate (mL min <sup>-1</sup> )	B	20	10	30	40
Air Flow rate (mL min <sup>-1</sup> )	A	800	200	500	1000
Recycling Liquid Flow rate (mL min <sup>-1</sup> )	L	10	5	20	30

572

573

**Table 2.** Taguchi's  $L_{16}(4^5)$  orthogonal array and mean results

Trial	Control factors and levels					Mean results of biomethane concentration				
	M	IC	B	A	L	CO <sub>2</sub> (%)	H <sub>2</sub> S (%)	O <sub>2</sub> (%)	N <sub>2</sub> (%)	CH <sub>4</sub> (%)
1	1	1	1	1	1	4.5	0.035	0.27	0.85	94.4
2	1	2	2	2	2	2.7	0.046	0.37	1.65	95.3
3	1	3	3	3	3	5.6	0.034	0.21	0.66	93.5
4	1	4	4	4	4	4.3	0.025	0.14	0.83	94.7
5	2	1	2	3	4	4.0	0.000	0.21	0.93	94.8
6	2	2	1	4	3	17.8	0.000	0.16	0.64	81.4
7	2	3	4	1	2	24.9	0.000	0.25	0.78	74.0
8	2	4	3	2	1	17.9	0.000	0.11	0.84	81.2
9	3	1	3	4	2	3.2	0.011	0.12	0.96	95.7
10	3	2	4	3	1	19.7	0.007	0.08	0.45	79.8
11	3	3	1	2	4	3.1	0.025	0.10	0.30	96.5
12	3	4	2	1	3	1.7	0.038	0.25	1.78	96.2
13	4	1	4	2	3	6.3	0.014	0.16	0.56	93.0
14	4	2	3	1	4	12.2	0.023	0.14	0.61	87.0
15	4	3	2	4	1	1.6	0.006	0.51	0.74	97.2
16	4	4	1	3	2	2.5	0.016	0.20	0.39	96.9

**Table 3.** ANOVA for the regular analysis

Factor	p Value				
	CO <sub>2</sub>	H <sub>2</sub> S	O <sub>2</sub>	N <sub>2</sub>	CH <sub>4</sub>
M	5.51×10 <sup>-35*</sup>	2.50×10 <sup>-7*</sup>	8.52×10 <sup>-3*</sup>	4.26×10 <sup>-3*</sup>	2.21×10 <sup>-36*</sup>
IC	1.01×10 <sup>-29*</sup>	7.04×10 <sup>-1</sup>	7.77×10 <sup>-2</sup>	2.92×10 <sup>-2*</sup>	3.55×10 <sup>-31*</sup>
B	2.62×10 <sup>-33*</sup>	1.39×10 <sup>-1</sup>	1.41×10 <sup>-5*</sup>	5.24×10 <sup>-7*</sup>	6.21×10 <sup>-34*</sup>
A	3.72×10 <sup>-20*</sup>	2.58×10 <sup>-2*</sup>	2.63×10 <sup>-1</sup>	9.43×10 <sup>-3*</sup>	1.75×10 <sup>-22*</sup>
L	6.75×10 <sup>-22*</sup>	2.48×10 <sup>-1</sup>	4.36×10 <sup>-2*</sup>	3.48×10 <sup>-2*</sup>	1.02×10 <sup>-23*</sup>

578

\*A significance level p&lt;0.05 was used to identify significant factors

579

**Figure 1.** Schematic diagram of the experimental plant used for the integral upgrading of biogas.

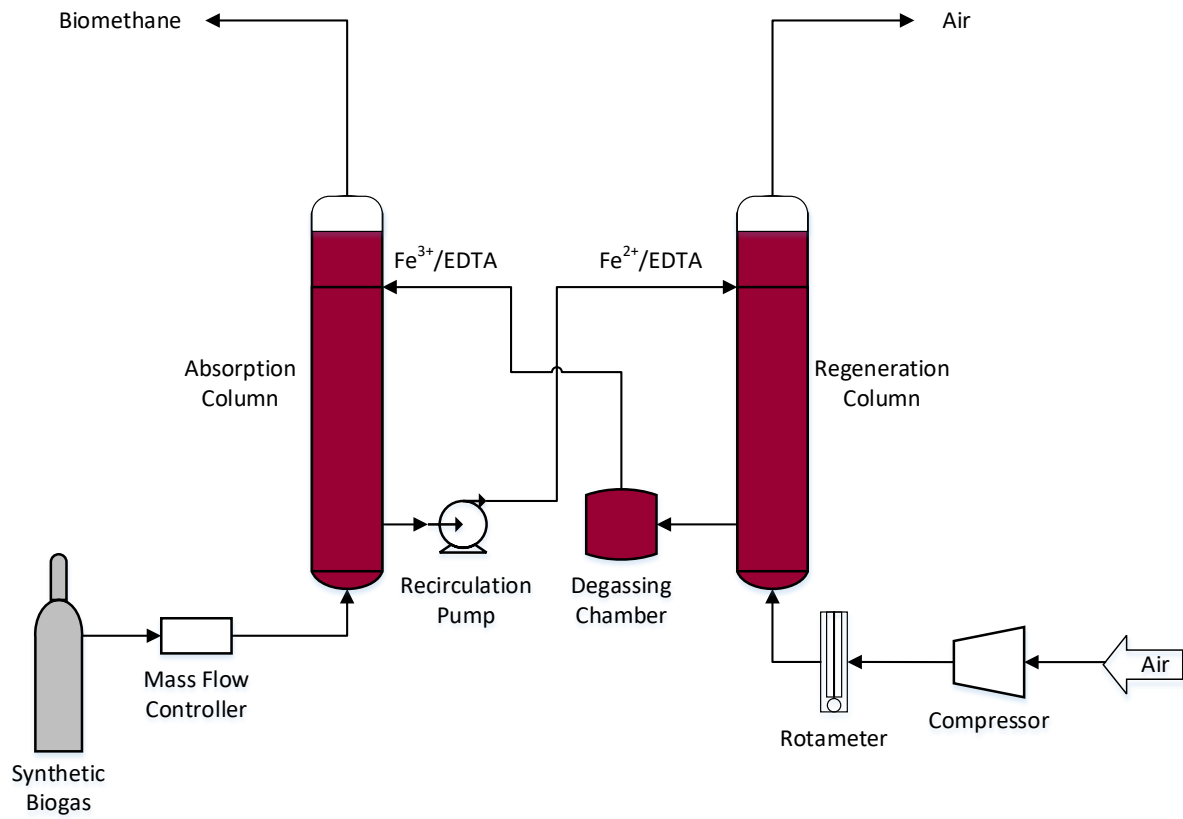


**Figure 2.** Influence of the control factors on the mean response of (a) CO<sub>2</sub> (■), (b) H<sub>2</sub>S (●), (c) O<sub>2</sub> (▲), (d) N<sub>2</sub> (□) and (e) CH<sub>4</sub> (○) concentration in the upgraded biogas.

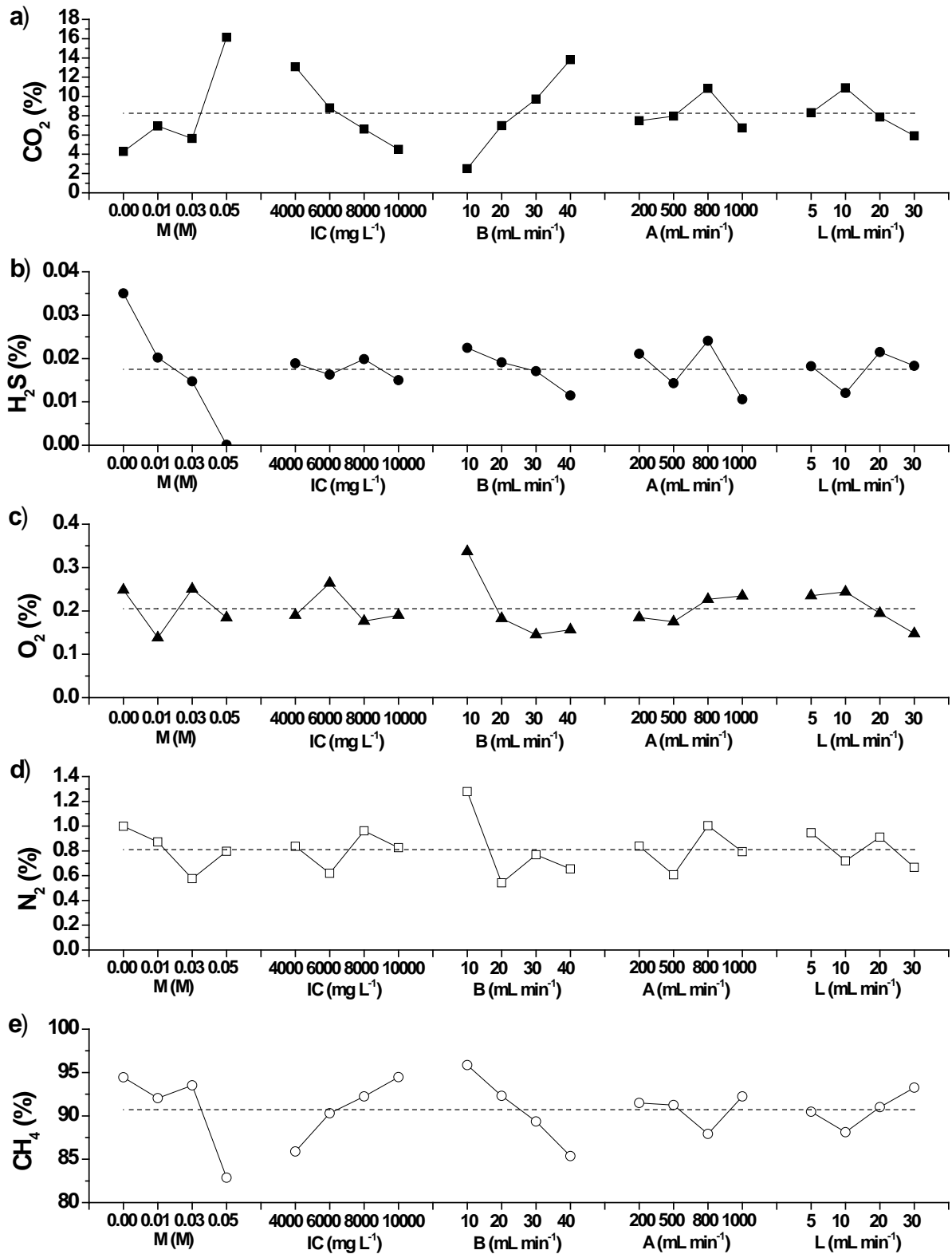




**Figure 3.** Effect of interactions between Fe/EDTA molarity and inorganic carbon

concentration ((■) 4000, (○) 6000, (▲) 8000 and (◇) 10000 mg L<sup>-1</sup>) on the concentrations of

(a) CO<sub>2</sub> and (b) H<sub>2</sub>S in the upgraded biogas.

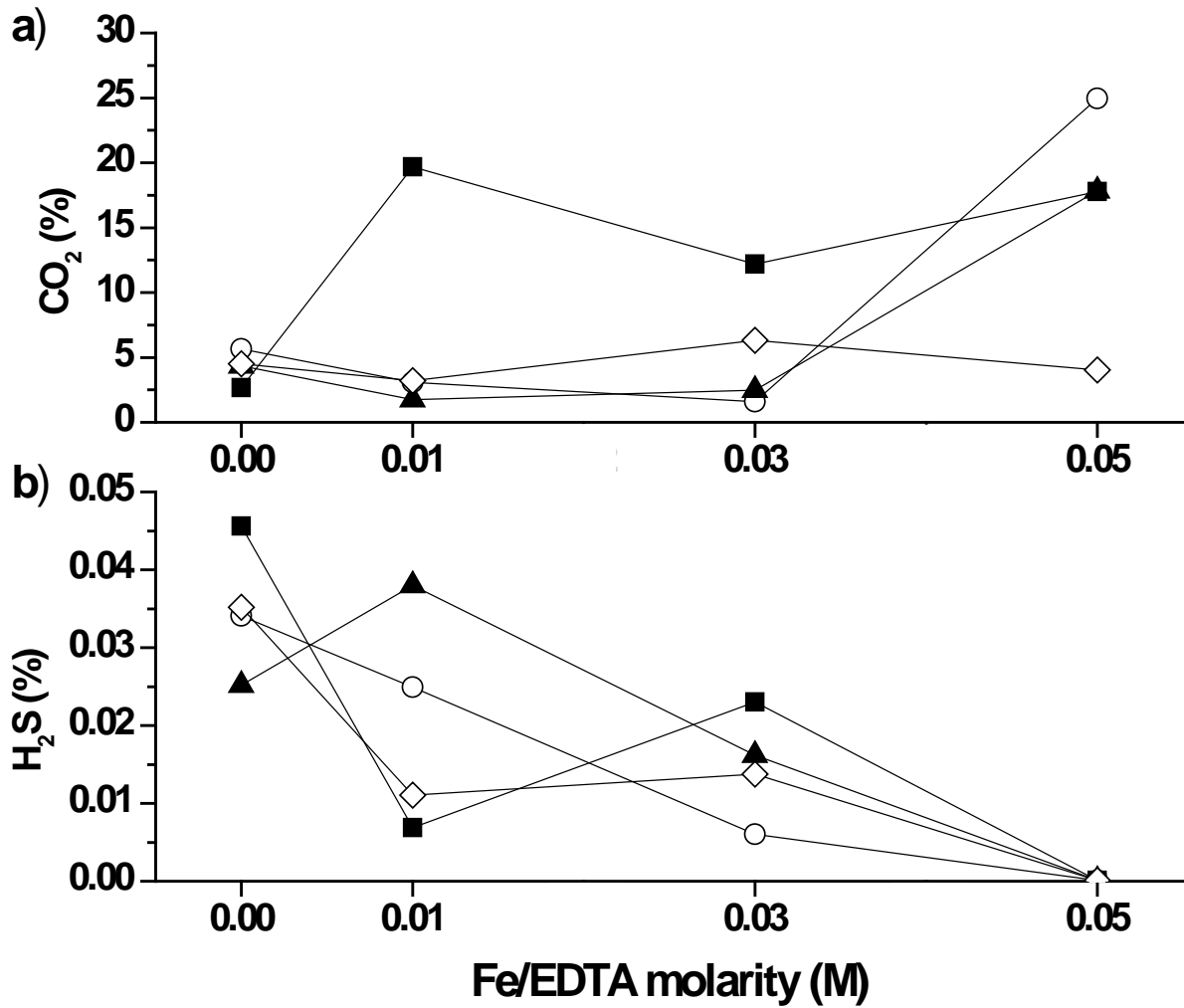


**Figure 4.** Time course of the concentration of (a) CO<sub>2</sub> (■), (b) H<sub>2</sub>S (●), (c) O<sub>2</sub> (▲), (d) N<sub>2</sub> (□) and (e) CH<sub>4</sub> (○) in the upgraded biogas.

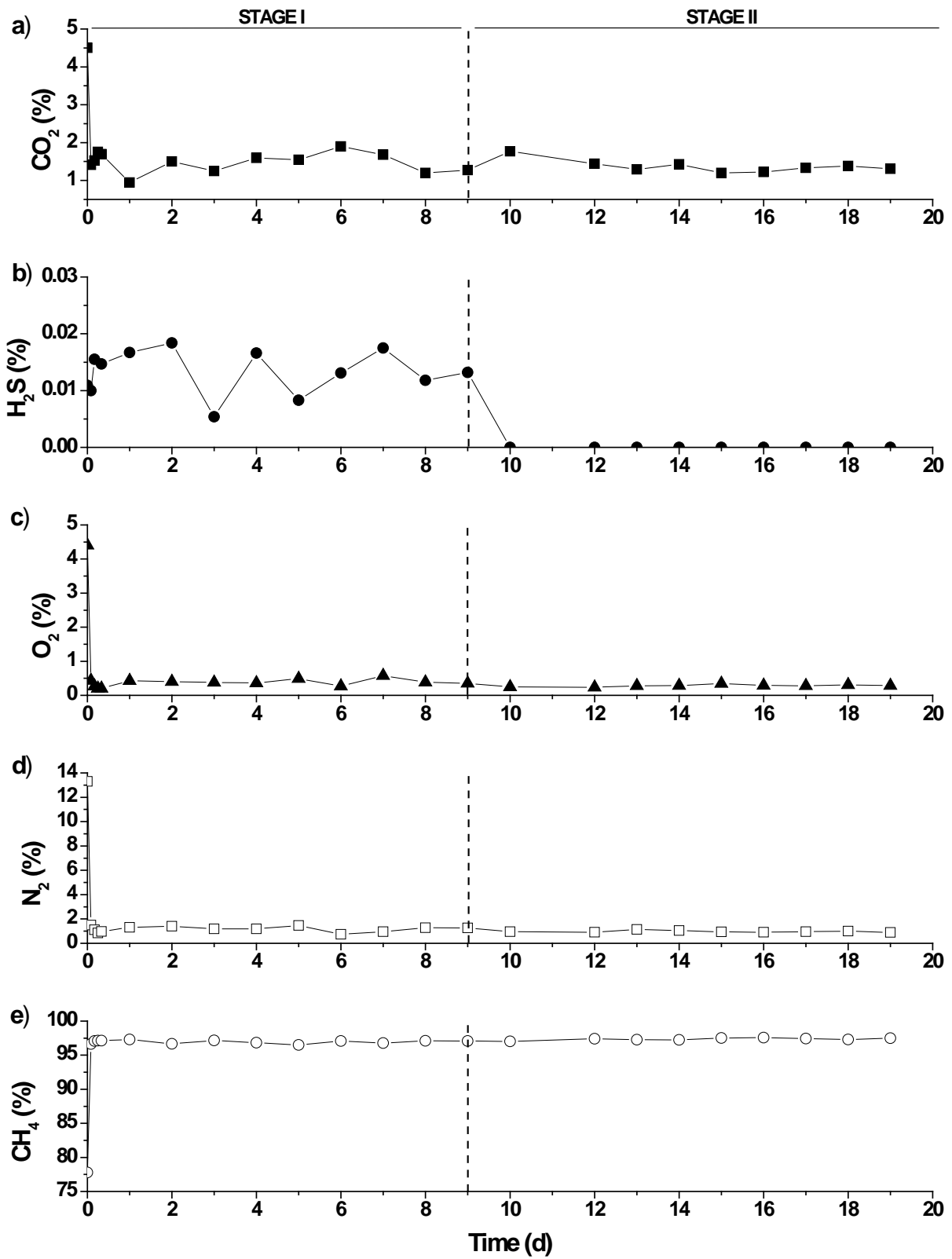


**Table 1.** Factors and levels for the optimization of biogas upgrading

<b>Factor</b>	<b>Acronym</b>	<b>Levels</b>			
		<b>1</b>	<b>2</b>	<b>3</b>	<b>4</b>
Fe/EDTA Molarity (M)	M	0.00	0.05	0.01	0.03
Inorganic Carbon Concentration (mg L <sup>-1</sup> )	IC	10000	4000	6000	8000
Biogas Flow rate (mL min <sup>-1</sup> )	B	20	10	30	40
Air Flow rate (mL min <sup>-1</sup> )	A	800	200	500	1000
Recycling Liquid Flow rate (mL min <sup>-1</sup> )	L	10	5	20	30

**Table 2.** Taguchi's L<sub>16</sub>(4<sup>5</sup>) orthogonal array and mean results

Control factors and levels						Mean results of biomethane concentration				
Trial	M	IC	B	A	L	CO <sub>2</sub> (%)	H <sub>2</sub> S (%)	O <sub>2</sub> (%)	N <sub>2</sub> (%)	CH <sub>4</sub> (%)
1	1	1	1	1	1	4.5	0.035	0.27	0.85	94.4
2	1	2	2	2	2	2.7	0.046	0.37	1.65	95.3
3	1	3	3	3	3	5.6	0.034	0.21	0.66	93.5
4	1	4	4	4	4	4.3	0.025	0.14	0.83	94.7
5	2	1	2	3	4	4.0	0.000	0.21	0.93	94.8
6	2	2	1	4	3	17.8	0.000	0.16	0.64	81.4
7	2	3	4	1	2	24.9	0.000	0.25	0.78	74.0
8	2	4	3	2	1	17.9	0.000	0.11	0.84	81.2
9	3	1	3	4	2	3.2	0.011	0.12	0.96	95.7
10	3	2	4	3	1	19.7	0.007	0.08	0.45	79.8
11	3	3	1	2	4	3.1	0.025	0.10	0.30	96.5
12	3	4	2	1	3	1.7	0.038	0.25	1.78	96.2
13	4	1	4	2	3	6.3	0.014	0.16	0.56	93.0
14	4	2	3	1	4	12.2	0.023	0.14	0.61	87.0
15	4	3	2	4	1	1.6	0.006	0.51	0.74	97.2
16	4	4	1	3	2	2.5	0.016	0.20	0.39	96.9

**Table 3.** ANOVA for the regular analysis

<b>Factor</b>	<b>p Value</b>				
	<b>CO<sub>2</sub></b>	<b>H<sub>2</sub>S</b>	<b>O<sub>2</sub></b>	<b>N<sub>2</sub></b>	<b>CH<sub>4</sub></b>
M	$5.51 \times 10^{-35*}$	$2.50 \times 10^{-7*}$	$8.52 \times 10^{-3*}$	$4.26 \times 10^{-3*}$	$2.21 \times 10^{-36*}$
IC	$1.01 \times 10^{-29*}$	$7.04 \times 10^{-1}$	$7.77 \times 10^{-2}$	$2.92 \times 10^{-2*}$	$3.55 \times 10^{-31*}$
B	$2.62 \times 10^{-33*}$	$1.39 \times 10^{-1}$	$1.41 \times 10^{-5*}$	$5.24 \times 10^{-7*}$	$6.21 \times 10^{-34*}$
A	$3.72 \times 10^{-20*}$	$2.58 \times 10^{-2*}$	$2.63 \times 10^{-1}$	$9.43 \times 10^{-3*}$	$1.75 \times 10^{-22*}$
L	$6.75 \times 10^{-22*}$	$2.48 \times 10^{-1}$	$4.36 \times 10^{-2*}$	$3.48 \times 10^{-2*}$	$1.02 \times 10^{-23*}$

\*A significance level  $p < 0.05$  was used to identify significant factors

1 **Optimization of a chemical scrubbing process based on a Fe-EDTA-**  
2 **carbonate based solvent for the simultaneous removal of CO<sub>2</sub> and H<sub>2</sub>S**  
3 **from biogas**

4 David Marín<sup>1, 2, 3</sup>, Marisol Vega<sup>2, 4</sup>, Raquel Lebrero<sup>1, 2</sup>, Raúl Muñoz<sup>\*1, 2</sup>

5 <sup>1</sup>Department of Chemical Engineering and Environmental Technology, School of Industrial Engineering,  
6 Valladolid University, Dr. Mergelina, s/n, 47011, Valladolid, Spain.

7 <sup>2</sup>Institute of Sustainable Processes, Dr. Mergelina, s/n, 47011, Valladolid, Spain.

8 <sup>3</sup>Universidad Pedagógica Nacional Francisco Morazán, Boulevard Centroamérica, Tegucigalpa, Honduras.

9 <sup>4</sup>Department of Analytical Chemistry, University of Valladolid, Campus Miguel Delibes, Paseo Belén 7,  
10 47011 Valladolid, Spain.

11  
12 \* Corresponding author: [mutora@iq.uva.es](mailto:mutora@iq.uva.es)

13  
14 **Table S1.** Biomethane composition for the orthogonal array

15 a)

Trial	Control factors and levels					Biomethane composition in steady state replicate 1				
	M	IC	B	A	L	CO <sub>2</sub> (%)	H <sub>2</sub> S (%)	O <sub>2</sub> (%)	N <sub>2</sub> (%)	CH <sub>4</sub> (%)
1	1	1	1	1	1	4.2	0.025	0.24	0.84	94.7
2	1	2	2	2	2	2.7	0.063	0.28	1.72	95.3
3	1	3	3	3	3	5.1	0.033	0.22	0.73	93.9
4	1	4	4	4	4	3.8	0.017	0.22	0.69	95.3
5	2	1	2	3	4	3.8	0.000	0.31	1.27	94.6
6	2	2	1	4	3	18.4	0.000	0.16	0.60	80.8
7	2	3	4	1	2	25.3	0.000	0.21	0.65	73.8
8	2	4	3	2	1	17.8	0.000	0.07	1.29	80.9
9	3	1	3	4	2	3.0	0.011	0.15	0.77	96.1
10	3	2	4	3	1	18.7	0.021	0.18	0.84	80.3
11	3	3	1	2	4	2.8	0.031	0.07	0.42	96.7
12	3	4	2	1	3	1.9	0.039	0.46	1.97	95.6
13	4	1	4	2	3	6.2	0.041	0.16	0.55	93.0
14	4	2	3	1	4	11.4	0.028	0.16	0.67	87.8
15	4	3	2	4	1	1.6	0.006	0.32	1.11	97.0
16	4	4	1	3	2	2.6	0.000	0.10	0.25	97.1

16

17

18

19 b)

Trial	Control factors and levels					Biomethane composition in steady state replicate 2				
	M	IC	B	A	L	CO <sub>2</sub> (%)	H <sub>2</sub> S (%)	O <sub>2</sub> (%)	N <sub>2</sub> (%)	CH <sub>4</sub> (%)
1	1	1	1	1	1	4.3	0.039	0.28	0.90	94.5
2	1	2	2	2	2	2.4	0.031	0.48	1.72	95.3
3	1	3	3	3	3	5.9	0.037	0.19	0.63	93.3
4	1	4	4	4	4	5.0	0.035	0.10	0.40	94.5
5	2	1	2	3	4	3.6	0.000	0.25	1.12	95.0
6	2	2	1	4	3	17.6	0.000	0.16	0.62	81.6
7	2	3	4	1	2	25.0	0.000	0.16	0.47	74.3
8	2	4	3	2	1	18.4	0.000	0.16	0.56	80.9
9	3	1	3	4	2	3.3	0.006	0.10	1.06	95.6
10	3	2	4	3	1	20.1	0.000	0.01	0.13	79.8
11	3	3	1	2	4	3.6	0.022	0.12	0.33	96.0
12	3	4	2	1	3	1.4	0.044	0.16	1.68	96.7
13	4	1	4	2	3	6.4	0.000	0.15	0.55	92.9
14	4	2	3	1	4	12.8	0.026	0.11	0.55	86.5
15	4	3	2	4	1	1.5	0.006	0.61	0.56	97.3
16	4	4	1	3	2	2.3	0.000	0.21	0.49	97.0

20

21 c)

Trial	Control factors and levels					Biomethane composition in steady state replicate 3				
	M	IC	B	A	L	CO <sub>2</sub> (%)	H <sub>2</sub> S (%)	O <sub>2</sub> (%)	N <sub>2</sub> (%)	CH <sub>4</sub> (%)
1	1	1	1	1	1	4.9	0.042	0.29	0.80	93.9
2	1	2	2	2	2	2.9	0.042	0.36	1.52	95.2
3	1	3	3	3	3	6.0	0.032	0.20	0.63	93.2
4	1	4	4	4	4	4.3	0.024	0.11	1.41	94.2
5	2	1	2	3	4	4.6	0.000	0.08	0.40	95.0
6	2	2	1	4	3	17.3	0.000	0.018	0.69	81.9
7	2	3	4	1	2	24.5	0.000	0.36	1.21	74.0
8	2	4	3	2	1	17.4	0.000	0.11	0.67	81.8
9	3	1	3	4	2	3.3	0.017	0.12	1.06	95.5
10	3	2	4	3	1	20.3	0.000	0.06	0.37	79.3
11	3	3	1	2	4	2.9	0.022	0.10	0.13	96.8
12	3	4	2	1	3	1.9	0.031	0.14	1.70	96.3
13	4	1	4	2	3	6.3	0.000	0.16	0.59	92.9
14	4	2	3	1	4	12.3	0.016	0.14	0.61	86.9
15	4	3	2	4	1	1.6	0.006	0.60	0.57	97.2
16	4	4	1	3	2	2.6	0.049	0.29	0.44	96.6

22

23

24

25 **Table S2.** Mean steady state pH for each experiment in the absorption column

Trial	Control factors and levels					Initial pH	Final pH
	M	IC	B	A	L		
1	1	1	1	1	1	9.25	8.80
2	1	2	2	2	2	9.24	8.75
3	1	3	3	3	3	9.24	8.96
4	1	4	4	4	4	9.24	8.73
5	2	1	2	3	4	9.23	8.80
6	2	2	1	4	3	9.26	7.60
7	2	3	4	1	2	9.22	7.91
8	2	4	3	2	1	9.22	8.01
9	3	1	3	4	2	9.25	8.90
10	3	2	4	3	1	9.23	8.04
11	3	3	1	2	4	9.23	8.79
12	3	4	2	1	3	9.25	9.00
13	4	1	4	2	3	9.22	8.67
14	4	2	3	1	4	9.22	8.21
15	4	3	2	4	1	9.22	8.87
16	4	4	1	3	2	9.22	8.91

26

27 **Models with interactions and quadratic effects**

28 The model equations for each design response using quadratic effects can be represented  
29 by equations (S1) to (S5).

30

$$31 \text{ CO}_2 (\%) = 4.621 + 1.752M - 1.938IC + 2.680B - 0.536L - 0.309M \times C +$$

$$32 0.645M \times B - 1.765B \times IC + 0.981M \times M + 1.141A \times A - 0.555L \times L \quad (\text{S1})$$

$$33 R^2 = 98.7\%$$

34

$$35 \text{ H}_2\text{S} (\%) = 0.0265 - 0.0072M - 0.0027B - 0.0012A + 0.0030L - 0.0002M \times$$

$$36 IC + 0.0022M \times B + 0.0030IC \times B - 0.0042A \times A + 0.0002L \times L \quad (\text{S2})$$

$$37 R^2 = 96.5\%$$



38

$$\begin{aligned} 39 \quad O_2 (\%) = & 0.220 - 0.003IC - 0.037B + 0.055A - 0.014L + 0.028M \times IC + \\ 40 \quad & 0.013M \times B + 0.013IC \times B - 0.006IC \times IC \end{aligned} \quad (S3)$$

$$41 \quad R^2 = 71.5\%$$

42

$$\begin{aligned} 43 \quad N_2 (\%) = & 0.600 - 0.089M + 0.039IC - 0.119B + 0.002L + 0.021IC \times IC + \\ 44 \quad & 0.069M \times M + 0.017M \times IC + 0.065M \times B + 0.006IC \times B \end{aligned} \quad (S4)$$

$$45 \quad R^2 = 52.2\%$$

46

$$\begin{aligned} 47 \quad CH_4 (\%) = & 94.34 - 1.66M + 1.91IC - 2.52B + 0.54L + 0.29MIC - 0.70M \times B + \\ 48 \quad & 1.70IC \times B - 1.06M \times M - 1.08A \times A + 0.57L \times L \end{aligned} \quad (S5)$$

$$49 \quad R^2 = 98.2\%$$

50